# Photodetachment and photofragmentation studies of semiconductor cluster anions

Y. Liu, Q.-L. Zhang, F. K. Tittel, R. F. Curl, and R. E. Smalley
*Departments of Chemistry and Electrical Engineering, Rice Quantum Institute, Rice University, Houston, Texas 77251*

(Received 18 July 1986; accepted 12 September 1986)

Silicon, germanium, and gallium arsenide negative cluster ions are produced by laser vaporization followed by free supersonic expansion. Electron affinities (EA) of the corresponding neutral clusters are roughly bracketed by measuring the fluence dependence for photodetachment from anions at discrete probe laser wavelengths (above the photodetachment threshold the dependence on fluence is linear, below it is quadratic). An even/odd alternation is found in the negative ion distribution with gallium arsenide clusters with an odd number of atoms having higher EA's than their even neighbors. This suggests that the surfaces of the even clusters are extensively restructured in a way which eliminates dangling chemical bonds. For $Ga_xAs_y$ with $x+y$ constant, EA increases with increasing ratio of $y$ to $x$. The EA of silicon increases smoothly with cluster size extrapolating towards the EA of bulk silicon. Photofragmentation studies show that, like the corresponding positive ions, silicon and germanium negative ions with 11 to 23 atoms fission into mainly 5 to 10 atom negative ions. $Si_{10}^-$ and $Ge_{10}^-$ are the favorite daughters suggesting the existence of a special structure for ten atoms.

## INTRODUCTION

Cluster models have been employed in theoretical treatments of semiconductor surfaces and defects for some years.[1-7] However, in this modeling the theorist had until recently no experimental checks in the form of properties of real isolated clusters. The development of techniques for producing supersonic cluster beams of refractory materials[8,9] has changed this situation, and several experimental studies of semiconductor cluster beams have appeared.[10-13] Both cluster ions[10,11] and neutral clusters[12,13] of semiconductors have been observed. More recently, a technique for studying semiconductor cluster ions produced upon condensation after laser vaporization by Fourier transform ion cyclotron resonanace has been developed.[14,15] The general conclusions of these studies are that Si and Ge clusters are easily fissioned into clusters of 5 to 11 atoms[10,12] while GaAs clusters fragment by loss of arsenic atoms[13] indicating some fundamental difference in chemical bonding. Two color two-photon ionization of Si and Ge clusters[12] indicated the presence of a reasonably long-lived (100 ns) intermediate excited state. A pronounced even/odd alternation in photoionization cross section of $Ga_xAs_y$ clusters[13] indicates that even clusters have fully paired singlet ground states with no dangling bonds. This view is supported by the observation[14] that the odd clusters of $In_xP_y^-$ are more intense than their even neighbors. A similar even/odd alternation in the intensities of Si negative ions produced by laser vaporization has also been reported.[11]

The ability to produce cold beams of cluster ions provides an exciting prospect for obtaining a wealth of detailed information for these systems because a particular ion can be mass selected for subsequent laser probing. Negative ions, in particular, have the attractive property of a low photodetachment threshold. This permits the study of competition between photodetachment and photofragmentation, and, in future work, should allow the convenient study of high resolution spectroscopy by resonance enhanced two-photon photodetachment.

In this paper, we describe photodetachment and photofragmentation of Si, Ge, and GaAs cold negative cluster ions. As detailed below, the fragmentation pattern of these ions again demonstrates the special nature of six to ten atom size clusters of Si and Ge. The fragmentation patterns of Si and Ge negative cluster ions are remarkably similar and colorful in their dependence upon cluster size. Even more interesting to us is that both one-photon photofragmentation and one-photon photodetachment are observed simultaneously for Si and Ge negative ion clusters with their relative importance depending strongly upon wavelength. The one-photon photodetachment thresholds of GaAs clusters (electron affinities of the neutrals) were studied as a function of cluster size and cluster composition. We find a pronounced even/odd alternation in EA with total number of atoms, but a monotonic change in EA with composition for a given total number of atoms, increasing with increasing As content as expected. The even/odd alternation in electron affinity is similar to the alternation in photoionization cross section of the neutral clusters observed previously.[13]

## EXPERIMENTAL

The semiconductor cluster ion apparatus used in this experiment is essentially identical to the one used for the photodetachment study of transition metal cluster ions carried out previously in this laboratory[16] except that here a semiconductor disk source[13] was used. Another difference from the previous study[16] is that the semiconductor cluster ions were produced by the vaporization laser only instead of by an excimer pulse directed into the nozzle. A detailed de-

 0021-9606/86/247434-08$02.10 

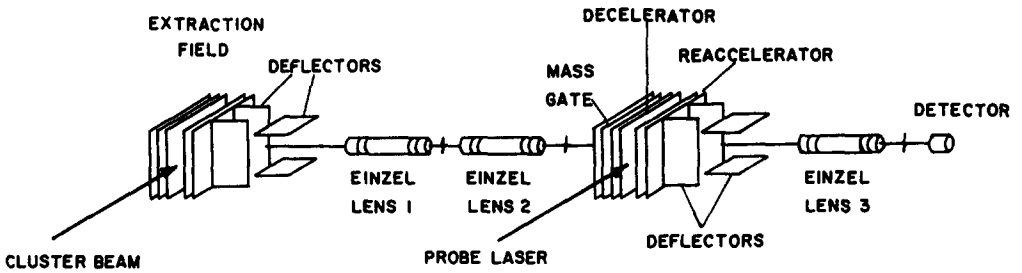


FIG. 1. Schematic of the tandem time-of-flight mass spectrometer. The extraction stack is composed of an array molybdenum-mesh gridded stainless steel electrodes (15 cm square) providing a two-stage acceleration field. The deceleration and reacceleration electrodes are similar.

scription of the apparatus was given previously,[16] but for purposes of orientation a schematic is given in Fig. 1.

In essence, refractory material is pulse laser vaporized into the He flow from a pulsed valve, the hot plasma stream is carried down a flow tube allowing condensation to clusters to take place and then expanded into a vacuum. After a free expansion, the supersonic molecular jet is skimmed into molecular beam and introduced into a second chamber which contains an extraction region where the negative ions are accelerated out of the beam by a pulsed two-stage electric field of 2 kV overall potential drop. The resulting ion beam is directed and focused along a field free flight tube. At the end of this tube, ions of a particular mass (flight time) are selected by a pulsed mass gate and decelerated into a chamber where they are laser probed via photodetachment and photodissociation processes. After interaction with this second probe laser, the resulting fragment anions and electrons are reaccelerated and focused along a second time-of-flight tube, and then detected by two MCP-409 microchannel plates.

The distribution and intensity of the negative ion cluster beam was found to depend sensitively upon the vaporization nozzle design. The most satisfactory nozzle design employed is depicted in Fig. 2. The second harmonic output of a *Q*-switched ND:YAG laser (30 mJ/pulse, 5 ns pulse width) is focused onto a 1 mm spot on a rotating target disk vaporizing the target surface and producing a very high temperature plasma. This plasma is entrained in the pulsed helium carrier gas flowing down a 2.5 mm diameter tube passing over the target which later expands into a 4 mm tube. This tube is 2 cm long with a lipped end and is followed by a 10 cm long 15° cone opening into the vacuum expansion chamber. Positive, negative, and neutral clusters are formed in this clustering and thermalization tube.

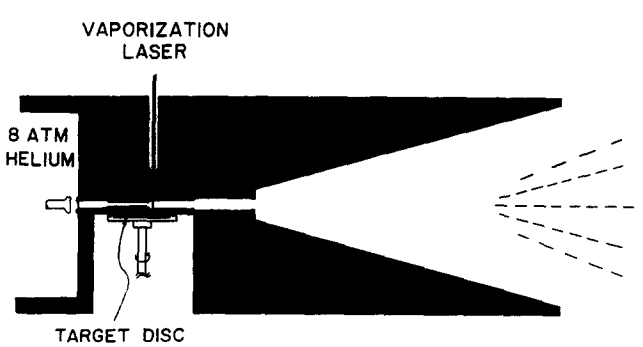


FIG. 2. Cross section of pulsed semiconductor cluster nozzle. In this study, the semiconductor disk is irradiated by a 532 nm laser (30 mJ/pulse, 5 ns pulse width). The ejected plasma is entrained in the pulsed helium (8 atm backing pressure) flowing down a 2.5 mm diam, 0.5 in. long channel which leads to the cluster formation/thermalization (4 mm diam, 2 cm long with a lipped end). The clusters formed are collimated by the 15 deg, 10 cm cone following free expansion.

## RESULTS AND DISCUSSION

### GaAs cluster anions

Figure 3(a) shows the typical mass spectrum for GaAs cluster anions generated in our apparatus. Atom and diatomic anions are hardly seen, probably because of their very low electron affinities or because the electron attachment process is inefficient. Upon close inspection of Fig. 3(a), an even/odd alternation in GaAs cluster anion intensities is apparent: odd anions are more abundant than the adjacent even ones. The same sort of even/odd alternation has been observed in the intensities of InP cluster anions.[14] In Fig. 3(b) we display the corresponding positive ion mass spectrum of GaAs clusters obtained by low fluence $F_2$ excimer

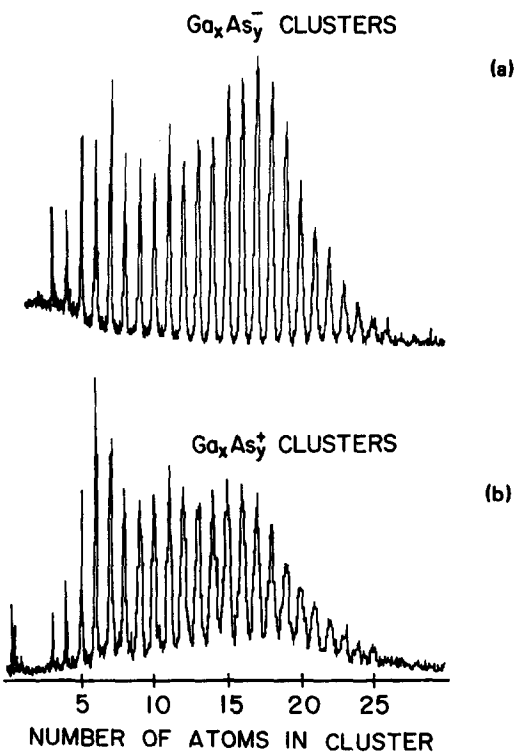


FIG. 3. Time-of-flight mass spectrum of GaAs clusters. The top spectrum (a) shows the GaAs anions produced by vaporization laser. The even/odd alternation is more obvious when one adjusts the deflector and einzel lens voltages to optimize the small cluster ions (3 to 15 atom size). The bottom trace (b) shows the mass spectrum of GaAs neutrals ionized by an $F_2$ excimer laser (7.9 eV) at 0.1 mJ cm$^{-2}$ fluence. The fact that the traces are so similar suggests that the traces reflect the actual GaAs cluster distributions.

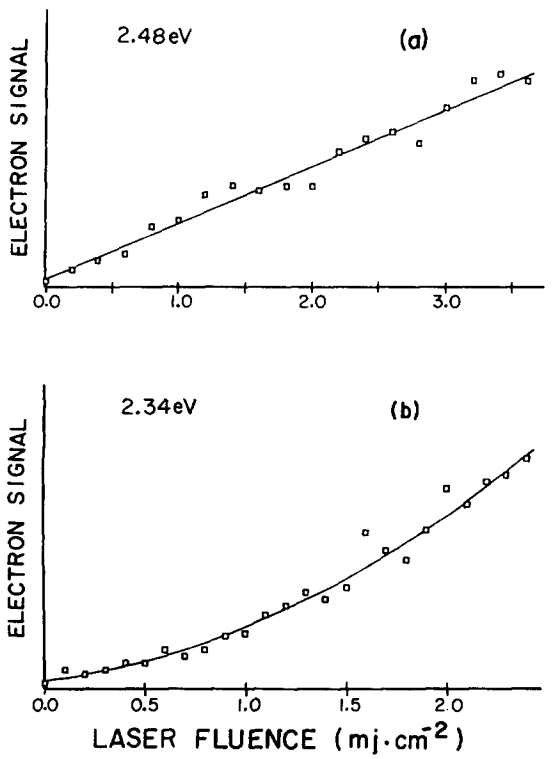


FIG. 4. Fluence dependence of the photodetachment of GaAs ten-atom cluster ions. (a) is linear in laser fluence and was obtained with a 2.48 eV laser. (b) is clearly quadratic and was taken at 2.34 eV photon energy. The probe laser firing time delay was carefully set so that the middle portion of the mass peak corresponding to a 1:1 Ga:As ratio was irradiated by the laser.

TABLE I. Estimates of the electron affinity for Si, Ge, and GaAs clusters obtained by fluence dependence of the laser photodetachment process from the cold negative cluster ion as a function of detachment photon energy.

| Cluster size $x$ | EA of $Si_x$ | EA of $Ge_x$ | EA of GaAs ($x$ atoms) |
|---|---|---|---|
| 5 | | | <1.82 |
| 6 | <2.34 | | <1.82 |
| 7 | <2.34 | | 2.19–2.34 |
| 8 | <2.34 | | <2.34 |
| 9 | 2.34–2.43 | | 2.48–3.00 |
| 10 | 2.48–2.70 | <2.91 | 2.34–2.48 |
| 11 | 2.48–2.70 | <2.91 | 2.48–2.82 |
| 12 | >3.00 | <2.91 | 2.48–3.00 |
| 13 | >3.00 | <2.91 | 2.82–3.00 |
| 14 | | >2.91 | 2.34–2.82 |
| 15 | >3.00 | >3.00 | 2.82–3.00 |
| 16 | | | 2.82–3.00 |
| 17 | | >3.51 | 3.00–3.51 |
| 18 | | >2.91 | <3.00 |
| 19 | | | 3.00–3.51 |
| 20 | | | <3.00 |
| 21 | | | 3.00–3.51 |
| 22 | | | <3.00 |
| 23 | | | 3.00–3.51 |
| 24 | | | 3.00–3.51 |
| 25 | | | 3.00–3.51 |
| 26 | | | 3.00–3.51 |
| 27 | | | 3.00–3.51 |
| 28 | | | 3.00–3.51 |
| 29 | | | >3.51 |
| 30 | | | 3.00–3.51 |

laser photoionization of the neutral clusters in the ionization region of the time-of-flight mass spectrometer (TOFMS).[13] It is obvious that the distributions are quite similar to each other, except that there are no even/odd alternations in the GaAs cation distribution of Fig. 3(b). All the GaAs clusters seen in Fig. 3(b) are one-photon ionized by the $F_2$ laser (157 nm). Also, an even/odd alternation similar to that of Fig. 3(a) was observed[13] for GaAs cations when ionized with a low fluence ArF laser at 193 nm, and was found to be due to the lower ionization potentials of odd clusters. (The odd clusters are one-photon ionized at 193 nm while the even are not.) It is likely that the even/odd alternation in GaAs anion intensity observed here could be due to the even/odd alternation in electron affinity with the odd ones having higher EA than their even neighbors. The photodetachment studies discussed below indeed verify such an alternation in electron affinity does exist.

Each peak shown in Fig. 3 corresponds to a certain *total* number of atoms and actually consists a number of peaks of $Ga_xAs_y$ with $x+y$ constant, which are not resolved in the figure. In the previous study, it was found that for small clusters ($x+y\sim6$) the distribution of $x$ and $y$ is more peaked than a binomial distribution, but that the distribution becomes more like the binomial with increasing cluster size being essentially binomial for $x+y\sim10$.

### *Electron affinity measurement*

As discussed by Zheng *et al.*,[16] there are two ways to estimate the EA. One is to determine the photodetachment threshold by scanning the photon frequency across the threshold region. The other is to detect the number of photons needed to detach the electrons by studying the dependence of the electron signal upon laser fluence. At photon energies close to the detachment threshold, it is difficult to determine whether the fluence dependence is linear or qua-

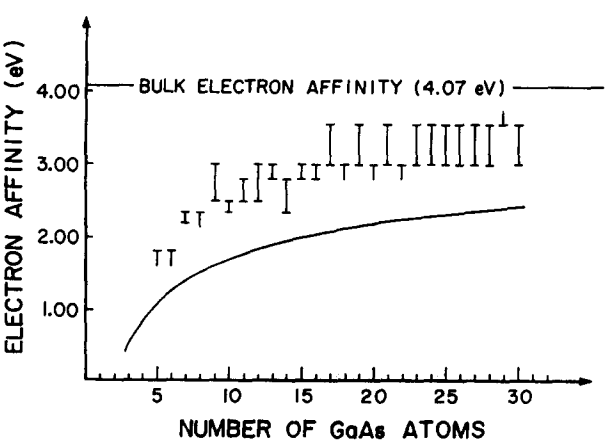


FIG. 5. Estimates of the electron affinity of GaAs clusters in the size range up to 30 atoms. In this plot, the firing time delay was adjusted so that the electron affinities corresponding to nearly stoichiometric GaAs were obtained. The curve shows the electron affinities as a function of GaAs cluster size calculated using Eq. (1). When the even/odd alternation in EA is smoothed out, both experimental brackets and the theoretical values appear to monotonically increase with cluster size gradually approaching the bulk value of 4.07 eV.

dratic. Therefore, by this method, one can only give a range for the adiabatic electron affinity which is bracketed by a definitely linear fluence dependence at one end (corresponding to the upper energy bound of the bracket) and a obviously nonlinear fluence dependence of positive curvature at the other end. The laser scanning method, on the other hand, seems to give a sharper value for the detachment threshold. However, the EA thus measured is a vertical, instead of adiabatic, electron affinity. The difference between this vertical EA and the adiabatic one is very sensitive to the internal temperature of the cluster ion and to the geometry change between the anion and corresponding neutral, which is unknown to us. Fortunately, Zheng *et al.*[16] found that both techniques gave roughly the same results for cold metal cluster anions. Therefore, we chose to use the simpler-to-implement fluence-dependence method. Figure 4 illustrates the fluence dependence of the intensity of electrons detached from GaAs ten-atom clusters. Figure 4(a) is taken with 2.48 eV energy photons and shows the linear dependence indicative of a one-photon process. Figure 4(b) is taken at 2.34 eV photon energy, and its quadratic dependence implies that electron detachment is two photon.

### *EA of GaAs as a function of cluster size*

We have roughly bracketed the EA's of various GaAs anions up to 30 atom size by using a few discrete laser wavelengths as depicted in Table I. In these measurements care was taken to irradiate GaAs clusters with approximately equal numbers of Ga and As atoms as we may expect that the Ga rich portion of each GaAs cluster with a given total number of atoms has lower EA than the As rich portion. Figure 5 demonstrates the resulting EA's obtained as a function of cluster size. We can see, in Fig. 5, the EA of clusters appears to monotonically increase with cluster size. The bulk EA[17] is 4.07 eV, and the EA of the clusters appears to be gradually approaching the bulk value with increasing cluster size.

Wood[18] proposed a model based on the classical electromagnetic theory to estimate the ionization potential of a cluster which can be readily modified for electron affinities. In his model, clusters are taken to be spherical conducting particles; an assumption which may not be appropriate for semiconductor particles, but which we make for the purpose of obtaining some prediction of cluster electron affinities. The resulting formula for EA is

$$\mathrm{EA} = \mathrm{EA}_0 - 5e^2/8R, \qquad (1)$$

where $\mathrm{EA}_0$ is the bulk electron affinity and $R$ the radii of the cluster sphere. The number density of bulk GaAs material is $2.21\times10^{22}$ GaAs molecules/cm$^3$ implying $R = (3N/2.21\times10^{22}\times4\pi)^{1/3}$, where $N$ is the number of GaAs pairs in this cluster. The calculated EA's from this model are plotted in Fig. 5 as the smooth curve. This curve might approach agreement with the experimental observations at large cluster size, but the agreement is not impressive. The large difference between the calculated EA and the experimental data for small clusters is understandable: this simple model is almost certainly not appropriate. In addition, because the added electron goes into a surface state, the bulk EA depends upon which surface plane is being approached by the electron.

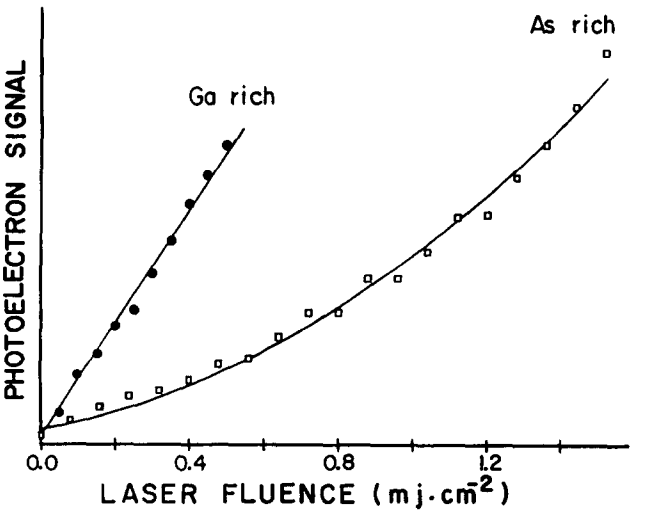


FIG. 6. Fluence dependence of the photodetachment of Ga rich and As rich GaAs seven-atom cluster ions with a 2.34 eV laser. The Ga rich portion shows a linear dependence upon laser fluence, whereas the As rich portion is quadratic. Note that the Ga rich clusters have lower EA's than the As rich clusters as is expected since As is more electronegative than Ga.

An even/odd alternation in EA is clear in Fig. 5. GaAs clusters with an odd total number of atoms have higher EA's than their neighboring even ones, and this alternation continues up to at least 30 atom size clusters. A similar even/odd alternation was observed in electron affinities of Cu clusters before in this lab.[16] Since both Ga and As have an odd number of valence electrons, odd GaAs clusters are odd-electron systems and the even clusters are even-electron system. A similar even/odd alternation in IP's of the neutral clusters has been observed,[14] and a model was proposed to explain this which stated that the even clusters had fully paired singlet ground states with no dangling bonds, but the odd clusters of necessity would have dangling bonds. This implies that odd clusters should have the unpaired electron in a nonbonding frontier orbital, and the even ones in a strongly bonding HOMO giving rise a higher ionization potential for even clusters. With respect to electron affinities of the neutrals, the extra electron adds for odd clusters into the half-filled nonbonding frontier orbital, while for even clusters it adds to a strongly antibonding LUMO, leading to lower electron affinities for the even clusters. Our experimental results are consistent with this prediction.

### *EA of Ga rich and As rich clusters*

By changing the firing time of the laser we can detach either the earlier or later part of a mass peak corresponding to the Ga rich and As rich part of the cluster, respectively. With the second harmonic output of a ND:YAG laser (532 nm) we found that, for GaAs clusters 7 and 8, the electrons of Ga rich anions were one-photon detached while that of As rich ones were two-photon detached, as shown in Fig. 6 for cluster 7. In cluster 9, all components required two 532 nm photons for detachment. The same experiment was repeated at 500 and 440 nm using higher clusters. We conclude that the Ga rich clusters have lower EA's than the As rich clusters. This conclusion is not surprising, since As is more electronegative than Ga.

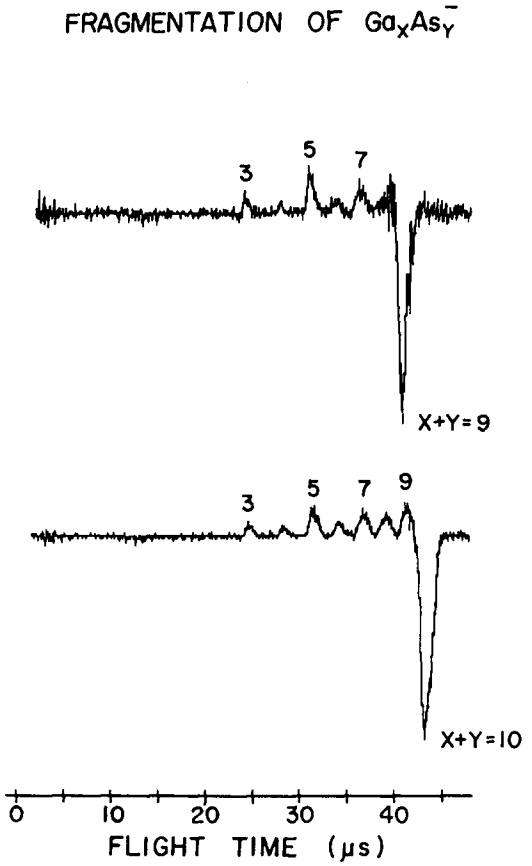


FIG. 7. Time-of-flight mass spectra of the photoproducts of laser irradiation of mass-selected cold GaAs cluster anions. The horizontal axis is the flight time of the anions from the photolysis region to the detector. The vertical scale is the difference between the ion signal seen when the photofragmentation laser was on and that seen when the laser was off. The selected parent ions were nine-atom GaAs anions for the top trace and ten-atom GaAs anions for the bottom trace. The photolysis laser was the second harmonic of the Nd:YAG (2.34 eV, 532 nm).

## Photodissociation of GaAs anions

Photodissociation processes were found to be quite competitive with photodetachment processes for GaAs negative ions. Usually, both electrons and fragmentation products were observed. Although the bond energies of the larger clusters are not known, the bonding energy of $Ga_2$ is only 1.43 eV, GaAs is 2.18 eV, and $As_2$ is 3.96 eV.[19] Except for $As_2$, these values are comparable to the detachment thresholds of the clusters. Unlike Si and Ge negative cluster ions, GaAs ions fragment by a nonfission pattern: one, two, or more atoms may be eliminated. There is, however, the same even/odd alternation in the fragmentation ion products: odd daughters are much more abundant than the even daughters. This is not surprising in that odd anions have higher electron affinities than the even ones. Figure 7 shows the fragmentation patterns of clusters 9 and 10 irradiated by a laser at 532 nm. It is possible that some of the fragment ions in Fig. 7 are, in fact, granddaughters produced by a two-photon process. The signal strengths are not adequate to study the fluence dependence.

## Si and Ge cluster anions

Figures 8(a) and 9(a) show the distributions of silicon

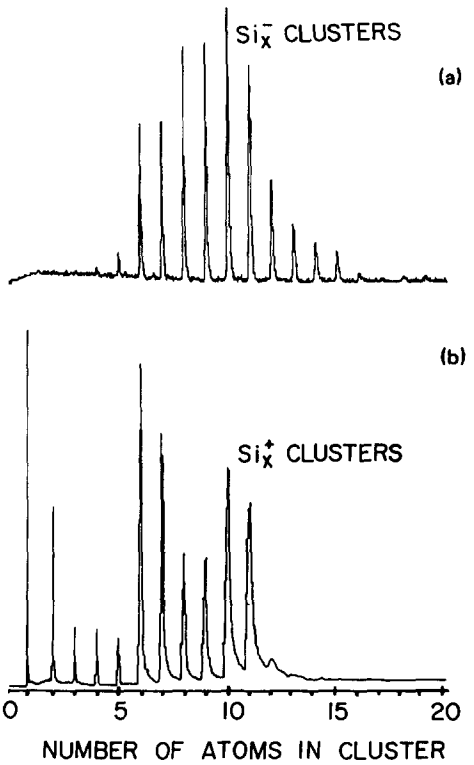


FIG. 8. Time-of-flight mass spectrum of Si clusters. (a) shows the Si negative ions produced by the vaporization laser. Note that there is no even/odd alternation in this picture under these nozzle conditions. (b) shows the mass spectrum of Si neutral clusters ionized with an ArF excimer laser. The similarity of these two traces suggests that Si ions in the six to ten atom size range are highly stable.

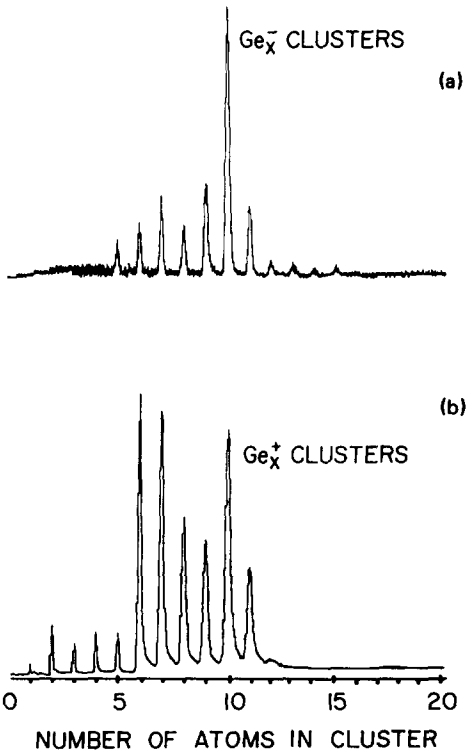


FIG. 9. Time-of-flight mass spectrum of Ge clusters. (a) shows the Ge negative ions produced by the vaporization laser. (b) shows the mass spectrum of Ge neutral clusters ionized with an ArF excimer laser. In both traces, six to ten atom size cluster ions are very stable. When the mass spectrum of the neutrals is obtained with $F_2$ laser ionization, $Ge_{10}^+$ is prominent like $Ge_{10}^-$ in (a) (Ref. 12).

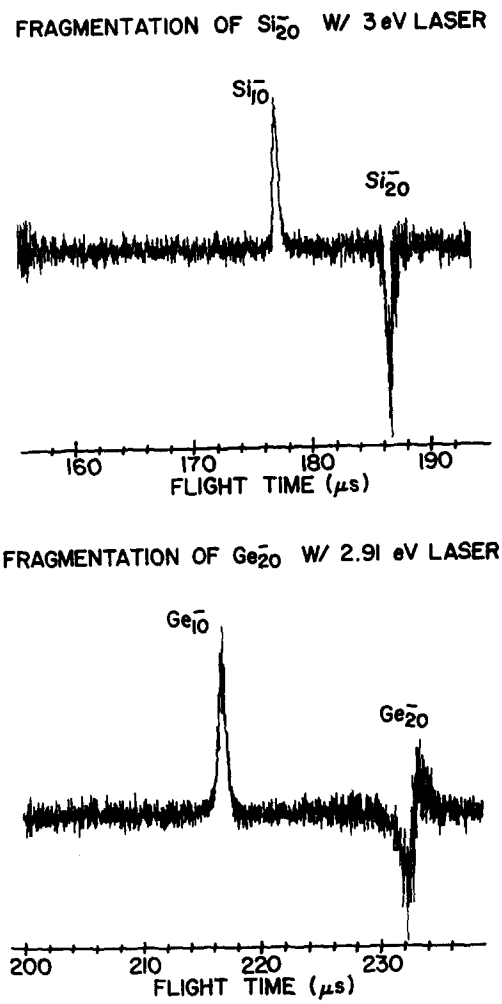


FIG. 10. Fragmentation patterns of $Si_{20}^-$ and $Ge_{20}^-$. The horizontal axis is the flight time from the ion extraction region to the detector. The top trace shows the selected parent ion $Si_{20}^-$ and its daughter ion $Si_{10}^-$ with a 3 eV laser. The bottom trace shows the dissociation of $Ge_{20}^-$ with product $Ge_{10}^-$ probed by a 2.91 eV laser. The parent ion $Ge_{20}^-$ signal is less than the daughter ion $Ge_{10}^-$ signal because of fluctuations in the cluster formation source.

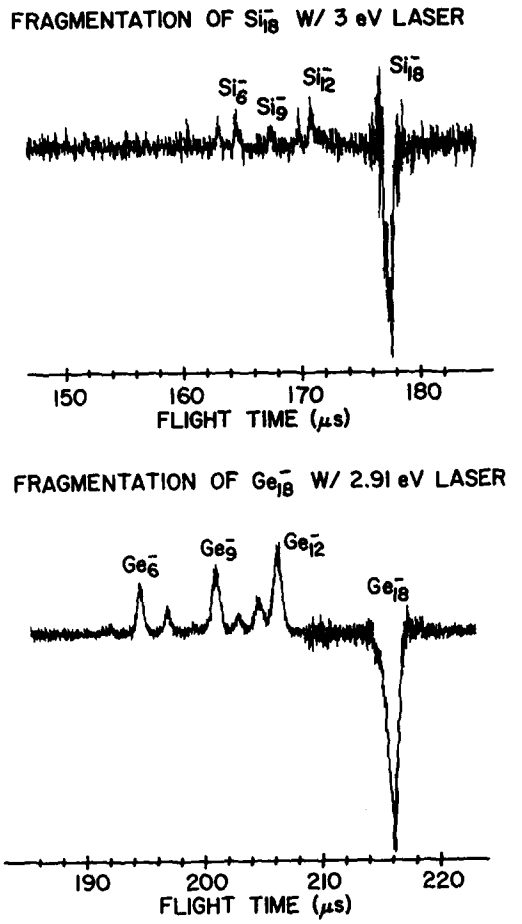


FIG. 11. Fragmentation patterns of $Si_{18}^-$ and $Ge_{18}^-$. The axes have the same meaning as in Fig. 10. The selected parent ion was $Si_{18}^-$ for the top trace and $Ge_{18}^-$ for the bottom trace. The probe laser energy was 3 eV for the top trace and 2.91 eV for the bottom. The products of these two parents are identical with the Ge anion exhibiting stronger fragmentation; however, the fragmentations are much more complicated than in the case of 20-atom parents. The electron signal is present in all of these fragmentation situations. However, in the other figures, we picked a small flight time range in order to show the fragmentation patterns more clearly. The $Si_6$ label refers to the left-most peak.

and germanium negative cluster ions. The negative ions were produced by the vaporization laser only. Also shown are the positive ion distributions obtained previously[12] by ionizing the neutral cluster beam with an ArF excimer. Generally, the four distributions are very similar, suggesting that ions in the six to ten atom size range may be very stable. The Ge distributions (Fig. 9) are more dissimilar from each other than the Si (Fig. 8). With low fluence $F_2$ laser ionization of the neutral cluster beam, $Ge_{10}$ is very prominent,[12] like the anion distribution [Fig. 9(a)].

Bloomfield *et al.*[11] reported an even/odd intensity alternation in the distribution of Si cluster anions. We have, on occasion, observed a similar even/odd intensity alternation in Si, but find that its existence depends rather sensitively upon the nozzle conditions and nozzle design.

### *Fragmentation*

As in the previous case[12] for neutrals, both silicon and germanium negative ion clusters fission into fragments containing five to ten atoms in striking contrast with metal[20] and GaAs clusters.[13] Figure 10 shows the fragmentation patterns of $Si_{20}^-$ and $Ge_{20}^-$ and Fig. 11 shows the fragmentation patterns of $Si_{18}^-$ and $Ge_{18}^-$. Comparing Figs. 10 and 11 with Fig. 7, one can see that Si and Ge ions tend to dissociate into a few channels and have one or two daughters.

Detachment and fragmentation compete with each other. Generally speaking, the bonding energies of $Si_x^-$ and $Ge_x^-$ are lower than the electron affinities. In certain ranges of laser energy, both are one-photon processes. In this situation the relative importance of the detachment channel and the fragmentation channels depends strongly upon wavelength. When the laser energy is just above the threshold, fragmentation signals dominate the electron signal; as the laser frequency is increased, the electron signals become larger than those of the fragmentation daughters. For example, for the reactions

$$Si_{11}^- + h\nu \rightarrow Si_5^- + Si_6^0, \quad (2)$$

$$Si_{11}^- + h\nu \rightarrow Si_{11}^0 + e^-, \quad (3)$$

the ratio of $e^-/Si_5^-$ changes from 0.25 to 5.5 as laser energy

TABLE II. Fragmentation channels of $Si_x^-$ and $Ge_x^-$.

| Parent size | Daughters $Si_y^-$ of $Si_x^-$ [a] | | Daughters $Ge_y^-$ of $Ge_x^-$ [a] | |
|---|---|---|---|---|
| $x$ | Size $y$ | Laser $\lambda$ (nm) | Size $y$ | Laser $\lambda$ (nm) |
| 9 | None | 532, 353, 414 | 5 | 426 |
| 10 | None | 532, 460, 440, 414, 353 | 4, 6, 5 | 426, 414 |
| 11 | **5**,[b] 4, 6 | 460, **440**, **414**, 353 | **5**,[b] 4, 6 | 440, **414** |
| 12 | **6**, 5 | **440**, 414, 353 | 6, 5 | 426 |
| 13 | 6, 7 | 414, 353 | **6**, 7 | **426**, 353 |
| 14 | 7, 10, 8 | 414, 353 | 7,[b] 10 | 426 |
| 15 | **9**, 5 | 440, **414**, 353 | 9, 5 | 426, 414 |
| 16 | 10 | 440, 414, 353 | 10 | 426 |
| 17 | 10 | 440, 353 | **10**, | **426**, 353 |
| 18 | 12, 6, 7, 9, 11 | 440, 414, 353 | 12, 9, 6, 11, 7, 10, 5 | 426 |
| 19 | 9, 10, 6 | 414, 353 | 9,[b] 6, 10 | 426 |
| 20 | **10** | 500, 440, **414**, 353 | 10 | 426 |
| 21 | 5, 9, 10, 11, 14, 15 | 414, 353 | 11, 5, 7, 10 | 426 |
| 22 | 10, 16, 6, 9, 5 | 353 | 16, 9, 10 | 426 |

[a] The daughters are listed in the order of decreasing intensity. Boldface type indicates that photofragmentation to this particular daughter is a one-photon process with the boldface wavelength laser.
[b] This daughter is of much higher intensity than the others.

changes from 2.82 to 3 eV. In the case of $Ge_{13}^-$, the competition is striking:

$$Ge_{13}^- + h\nu \rightarrow Ge_6^- + Ge_7^0 \quad (4)$$

$$\rightarrow Ge_6^0 + Ge_7^- \quad (5)$$

$$\rightarrow e^- + Ge_{13}^0, \quad (6)$$

$e^-/Ge_6^-$ changes from 0.07 to 6.8 as the photon energy increases from 2.91 to 3.51 eV. Presumably, if the laser energy is much larger than both $D_e$ and EA, electron detachment will be totally dominant.

With these fragmentations there are two new types of two-photon processes in addition to the more usual two-photon process in which the first photon excites a bound intermediate state: upon absorption of the first photon, the cluster first fragments and then either the electron can one-photon detach from the daughter even though detachment from the parent is below threshold or the daughter ion can fragment again producing a granddaughter ion. The former can make determination of the detachment threshold difficult although the fluence dependence should remain quadratic. In the latter case, the granddaughter may be mistaken for a daughter ion, particularly when the signals are too weak to measure their fluence dependence. Therefore, in observing the fragmentation of Si and Ge anions, some care must be taken to avoid two-photon processes.

Table II lists the observed fragmentation channels for Si and Ge negative clusters up to $n = 22$. There is no dependence of the relative intensities of the daughter ions upon the frequency of the probe laser in the range of our study. For example, $Si_{20}^-$ produces only $Si_{10}^-$ when probed at 500, 440, 414, or 353 nm wavelength. Generally, Si and Ge exhibit the same channels with a few exceptions although the relative intensities of daughter ion peaks are not equal between Si and Ge.

The most striking difference between $Si_x^-$ and $Ge_x^-$ is in the fragmentation of the nine and ten atom cluster anions. $Si_{10}^-$ is not dissociated at 532, 460, 440, 414, or 353 nm while in contrast, $Ge_{10}^-$ fragments at 426, 414, 353, nm. $Si_9^-$ is very stable, however, $Ge_9^-$ has a daughter ion $Ge_5^-$ at 426 nm. The most likely reason for this behavior is that the bonding energies of $Si_9^-$ and $Si_{10}^-$ are higher than those of $Ge_9^-$ and $Ge_{10}^-$, respectively, although another possibility is that detachment could completely dominate fragmentation for the Si species.

Some negative ions of Si and Ge produce only negative ions containing ten atoms while other ions produce several daughters as can be seen in Table II. For example, $Ge_{17}^-$ always fragments into $Ge_{10}^-$; however, $Ge_{18}^-$ produces daughter ions of 5, 6, 7, 9, 10, 11, and 12 atoms independent of laser frequency. Perhaps the explanation for this behavior may be found in large changes in the structure of the cluster with cluster size. Generally, it seems that the ten-atom ion is a favorite daughter and the ten-atom parent ion is more stable than other ions.

This conclusion does present some difficulties. Photofragmentation of $Si_{22}^-$ produces $Si_{10}^-$, $Si_{16}^-$, $Si_6^-$, $Si_9^-$, and $Si_6^-$ in that order of intensity. The simplest view of the fragmentation which produces $Si_{10}^-$ would be that it is a binary fission:

$$Si_{22}^- + h\nu \rightarrow Si_{10}^- + Si_{12}^0. \quad (7)$$

The electron affinity of $Si_{10}$ is less than that of $Si_{12}$ making the exit channel leading to $Si_{12}^-$ and $Si_{10}^0$ lower in energy. When the fragments are separating, an electron can easily tunnel between the fragments ensuring that this lower energy channel is accessible, and statistical arguments imply that it should dominate. Perhaps, instead of $Si_{12}^0$, smaller neutral fragments are formed. Unfortunately, we are not able to see the neutral fragments produced.

### *Electron affinities*

The electron affinities of Si and Ge clusters have been explored but not as carefully as those of GaAs. The information we have is shown in Table I. Because of our difficulty in

understanding the preferred fragmentation and because $Si_{10}^-$ is such a stable species, of most interest to us is the electron affinity of $Si_{10}$. We expected $Si_{10}$ to have an unusual small EA, but, in fact, the EA of $Si_{10}$ is quite normal being very close to that of $Si_{11}$. Indeed, when the general trends are considered, it appears $Si_{11}$ is abnormal in that it has an EA too low in comparison with $Si_{12}$.

## SUMMARY AND CONCLUSION

Electron affinities of GaAs, Si, and Ge clusters have been roughly determined as a function of cluster size for the first time. Generally, it was found that the EA increases with cluster size in a manner approaching that predicted by a simple electrostatic model. For GaAs clusters, the EA exhibits an alternating behavior between even and odd clusters with the EA of the odd larger. This is evidence for cluster structures without dangling bonds for the even clusters.

In contrast with GaAs and metal clusters, Si and Ge cluster ions (both positive and negative) fragment by fissioning. The fragmentation pathways have been determined and are highly colorful, perhaps reflecting large changes is structure with cluster size. For Si and Ge, photodetachment and photofragmentation occur simultaneously by a one-photon process in certain wavelength ranges. Generally, detachment becomes dominant at high photon energy.

## ACKNOWLEDGMENTS

The authors are grateful to Dr. M. C. Smayling of Texas Instruments Inc. for supplying the semiconductor wafers used in this study. We would also like to express our appreciation to James Heath, Sean O'Brien, Lan-Sun Zheng, and Philip Brucat for their help and advice. This work was supported by Contract DAAG 29-85-K-0029 of the U.S. Army Research Office. Portions of this work were also supported by grants from the Robert A. Welch Foundation.

[1] (a) C. A. Swarts, T. C. McGill, and W. A. Goddard III, Surf. Sci. **110,** 400 (1981); (b) C. A. Swarts, W. A. Goddard III, and T. C. McGill, J. Vac. Sci. Technol. **19,** 360, 551 (1981).
[2] W. H. Lamfried, and R. Strehlow, Phys. Status Solidi B **110,** K79 (1982).
[3] G. DeMeyer, R. Hoogewijs, W. Lambrecht, J. Vennik, and G. Dalmai, Surf. Sci. **106,** 498 (1981).
[4] B. K. Agrawal, Phys. Rev. B **23,** 2995 (1981).
[5] A. Fazzio, J. Leite, and M. DeSiquiera, J. Phys. C **12,** 513, 3496 (1979).
[6] (a) N. Nishida, Solid State Commun. **28,** 551 (1979); (b) Surf. Sci. **72,** 589 (1978).
[7] J. E. Lowther, J. Phys. C **9,** 2519 (1976).
[8] D. E. Powers, S. G. Hansen, M. E. Geusic, A. C. Puiu, J. B. Hopkins, T. G. Dietz, M. A. Duncan, P. R. R. Langridge-Smith, and R. E. Smalley, J. Phys. Chem. **86,** 2256 (1982).
[9] J. B. Hopkins, P. R. R. Langridge-Smith, M. D. Morse, and R. E. Smalley, J. Chem. Phys. **78,** 1627 (1983).
[10] L. Bloomfield, R. Freeman, and W. L. Brown, Phys. Rev. Lett. **534,** 2246 (1985).
[11] L. Bloomfield, M. E. Geusic, R. Freeman, and W. L. Brown, Chem. Phys. Lett. **121,** 33 (1985).
[12] J. R. Heath, Y. Liu, S. C. O'Brien, Q-L. Zhang, R. F. Curl, F. K. Tittel, and R. E. Smalley, J. Chem. Phys. **83,** 5520 (1985).
[13] S. C. O'Brien, Y. Liu, Q. Zhang, J. R. Heath, F. K. Tittel, R. F. Curl, and R. E. Smalley, J. Chem. Phys. **84,** 4074 (1986).
[14] V. E. Bondybey, W. D. Reents, and M. L. Mandich, J. Chem. Phys. (to be published).
[15] R. B. Knight, R. A. Walch, S. Foster, T. A. Miller, S. L. Mullen, and A. G. Marshall, Chem. Phys. Lett. **129,** 331 (1986).
[16] L.-S. Zheng, C. M. Karner, P. J. Brucat, S. H. Yang, C. L. Pettiette, M. J. Craycraft, and R. E. Smalley, J. Chem. Phys. **85,** 1681 (1986).
[17] S. M. Sze, *Physics of Semiconductor Devices* (Wiley, New York, 1969).
[18] D. N. Wood, Phys. Rev. Lett. **46,** 749 (1981).
[19] K. P. Huber and G. H. Herzberg, *Constants of Diatomic Molecules* (Van Nostrand Reinhold, New York, 1979).
[20] P. J. Brucat, L.-S. Zheng, C. L. Pettiette, S. Yang, and R. E. Smalley, J. Chem. Phys. **84,** 3078 (1986).